Title
Pacific and Atlantic controls of the relationship between Mainland Southeast Asia and East China interannual precipitation variability

Permalink
https://escholarship.org/uc/item/1414c9mq

Journal
Climate Dynamics, 54(9-10)

ISSN
0930-7575

Authors
Wang, Jessica K
Yu, Jin-Yi
Johnson, Kathleen R

Publication Date
2020-05-01

DOI
10.1007/s00382-020-05227-0

Supplemental Material
https://escholarship.org/uc/item/1414c9mq#supplemental

Copyright Information

Peer reviewed

The changing impact of El Niño on US winter temperatures

Jin-Yi Yu,[1] Yuhao Zou,[1] Seon Tae Kim,[1] and Tong Lee[2]

[1] In this study, evidence is presented from statistical analyses, numerical model experiments, and case studies to show that the impact on US winter temperatures is different for the different types of El Niño. While the conventional Eastern-Pacific El Niño affects winter temperatures primarily over the Great Lakes, Northeast, and Southwest US, the largest impact from Central-Pacific El Niño is on temperatures in the northwestern and southeastern US. The recent shift to a greater frequency of occurrence of the Central-Pacific type has made the Northwest and Southeast regions of the US most influenced by El Niño. It is shown that the different impacts result from differing wave train responses in the atmosphere to the sea surface temperature anomalies associated with the two types of El Niño. **Citation:** Yu, J.-Y., Y. Zou, S. T. Kim, and T. Lee (2012), The changing impact of El Niño on US winter temperatures, *Geophys. Res. Lett.*, *39*, L15702, doi:10.1029/2012GL052483.

1. Introduction

[2] The increasing recognition that there are two different flavors or types of El Niño events [e.g., *Wang and Weisberg*, 2000; *Trenberth and Stepaniak*, 2001; *Larkin and Harrison*, 2005a, 2005b; *Yu and Kao*, 2007; *Ashok et al.*, 2007; *Kao and Yu*, 2009; *Kug et al.*, 2009] offers the research community a new way to consider interannual sea surface temperature (SST) variability in the tropical Pacific and to rethink how the type of El Niño and its impacts may change as the climate changes. While El Niño is traditionally recognized as a warming of the sea surface in the eastern-to-central equatorial Pacific, it has been noticed that El Niño events with warming confined to the international dateline region can also occur. This flavor or type of El Niño has been referred to as the Central Pacific (CP) El Niño [*Yu and Kao*, 2007; *Kao and Yu*, 2009], Date Line El Niño [*Larkin and Harrison*, 2005a], El Niño Modoki [*Ashok et al.*, 2007], or warm pool El Niño [*Kug et al.*, 2009], while the conventional El Niño is referred to as the Eastern-Pacific (EP) type [*Yu and Kao*, 2007; *Kao and Yu*, 2009]. During the past few decades, more of the El Niño events have been of the CP type [*Ashok et al.*, 2007; *Kao and Yu*, 2009; *Kug et al.*, 2009; *Lee and McPhaden*, 2010]. Moreover, since the start of the 21st century, most of the El Niño events have been of the CP type, including the 2002/03, 2004/05, and 2009/10 events. The

tropical Pacific seems to be entering a state in which the preferred flavor of El Niño is the CP type.

[3] The El Niño impact on US winter temperatures is traditionally characterized as a north-south dipole pattern, in which warmer-than-normal temperatures are found over the northern states and colder-than-normal temperatures over the southern states [e.g., *Ropelewski and Halpert*, 1986]. However, the classical view of El Niño impacts on the United States (US) climate does not consider the existence of different types of El Niño. Therefore we may raise a question: How is the emergence of the CP El Niño going to change the El Niño impact on US winter temperatures, which has important socio-economic implications? The atmospheric response to tropical sea surface temperature (SST) anomalies can be sensitive to their exact locations [e.g., *Mo and Higgins*, 1998; *Hoerling and Kumar*, 2003; *Alexander et al.*, 2002; *Barsugli and Sardeshmukh*, 2002; *DeWeaver and Nigam*, 2004]. The classical view of the El Niño impact on the US may be a mixture of the impacts from the EP and the CP El Niños that may evolve as El Niño characteristics change on multi-decadal and longer time scales [e.g., *Mo*, 2010]. The possibly different impacts produced by these two types of El Niño can be a source of uncertainty in the prediction of El Niño impacts on US climate. The specific region of the US that is most vulnerable to the influence of each type of El Niño has yet to be examined. In this study, we conduct statistical analyses with observational data, numerical experiments with a forced atmospheric general circulation model (AGCM), and case studies with major El Niño events since 1950 to show that the impacts produced by the CP and EP types of El Niño on US winter temperatures are different from the classical view and that the El Niño impacts are indeed changing.

2. Data and Analysis Methods

[4] For the observational analyses, SSTs from National Oceanic and Atmospheric Administration (NOAA)'s Extended Reconstructed Sea Surface Temperature (ERSST) V3b dataset [*Smith and Reynolds*, 2003] and surface air temperatures and 500 mb geopotential heights from National Centers for Environmental Prediction–National Center for Atmospheric Research (NCEP–NCAR) Reanalysis [*Kistler et al.*, 2001] were used. Monthly SST, surface air temperature, and 500 mb geopotential height anomalies from 1950 to 2010 were analyzed. In this study, anomalies are defined as the deviations from the 1971–2000 climatology.

[5] A regression-Empirical Orthogonal Function (EOF) analysis [*Kao and Yu*, 2009; *Yu and Kim*, 2010] is used to identify the CP and EP types of El Niño from the monthly SST data. In this method, the SST anomalies regressed with the Niño1+2 (0°–10°S, 80°W–90°W) SST index were removed before the EOF analysis was applied to obtain the

[1]Department of Earth System Science, University of California, Irvine, California, USA.
[2]Jet Propulsion Laboratory, California Institute of Technology, Pasadena, California, USA.

Corresponding author: J.-Y. Yu, Department of Earth System Science, University of California, Irvine, CA 92697-3100, USA. (jyyu@uci.edu)
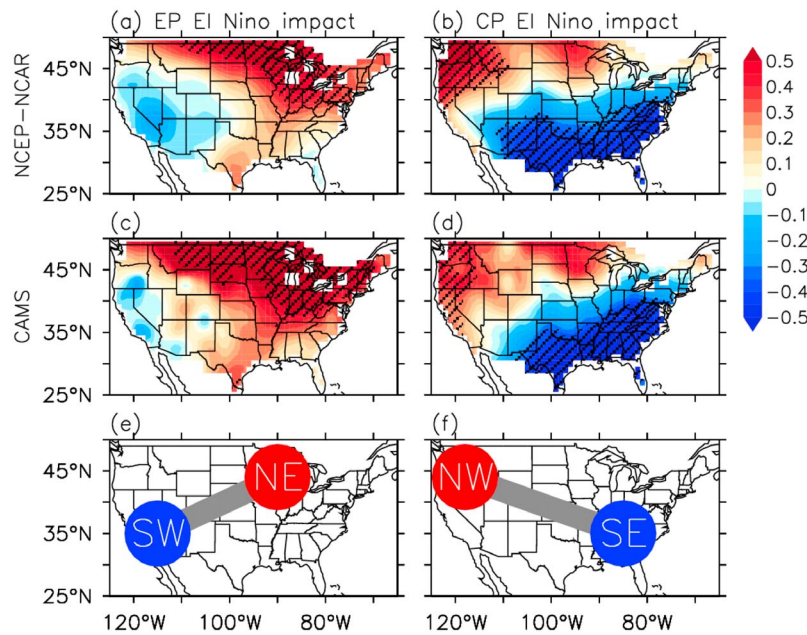
Figure 1. Observed US winter (January–February–March) surface air temperature anomalies regressed onto the (left) EP and (right) CP El Niño indices. Observations correspond to (a, b) the NCEP-NCAR reanalysis and (c, d) the CAMS air temperature data set. Regression coefficients significant at the 90% confidence level based on the student-t test are shaded. (e, f) Schematic diagrams of the EP and CP El Niño impacts on US winter surface air temperatures are also shown.

spatial pattern of the CP El Niño. The regression with the Niño1+2 index was used as an estimate of the influence of the EP El Niño and was removed to better reveal the SST anomalies associated with the CP El Niño. Similarly, we subtracted the SST anomalies regressed with the Niño4 (5°S–5°N, 160°E–150°W) index (i.e., representing the influence of the CP El Niño) before the EOF analysis was applied to identify the leading structure of the EP El Niño. The leading EOF modes obtained from this analysis represent the typical SST anomaly patterns of these two types of El Niño and the associated principal components represent the El Niño strengths and are defined as the CP El Niño index and the EP El Niño index, respectively.

3. Results

[6] By separately regressing winter (January–February–March; JFM) surface air temperature anomalies to the EP and CP El Niño indices, we show in Figures 1a and 1b that the El Niño impacts on US winter temperatures are different between these two types. Neither of the impacts resembles the classical warm-north, cold-south anomaly pattern. During EP El Niño events, positive winter temperature anomalies are concentrated mostly over the northeastern part of the US (particularly over the Great Lakes region) and negative anomalies are most obvious over the southwestern states. During CP El Niño events, the warm anomalies are located in northwestern US and the cold anomalies are centered in the southeastern US. The US temperature impact patterns are rotated by about 90 degrees between these two types of El Niño. We note that adding these two impact patterns together results in a pattern that resembles the classical warm-north, cold-south pattern. It indicates that the classical impact view is a mixture of the impacts of the two types of El Niño. We also repeated the regression analysis with a

surface air temperature anomaly data set from the Climate Anomaly Monitoring System (CAMS) [*Ropelewski et al.*, 1984] from the Climate Prediction Center of the NCEP. The CAMS air temperature is on a 2.0° × 2.0° grid and available from 1950 onward. As shown in Figures 1c and 1d, the results are similar to those produced with the NCEP-NCAR reanalysis.

[7] To further confirm that the different impacts revealed by the regression analysis are due to the different SST forcing from the two types of El Niño, forced experiments were performed with version 4 of the Community Atmosphere Model (CAM4) from NCAR. Three sets of ensemble experiments were conducted with a T42 (64 × 128) Euler spectral resolution of CAM4: a control run, an EP run, and a CP run. In the control run, climatological and annually-cycled SSTs are used as the boundary condition to force CAM4. For the EP (CP) run, the CAM4 is forced by SSTs constructed by adding together the climatological SSTs and the SST anomalies of the EP (CP) El Niño. For each of the runs, a 10-member ensemble of 22-month integrations was conducted with the El Niño SST anomalies evolved from the developing phase, peak phase, to decaying phase. The peak phases of the SST anomalies were placed in December of Year 1 of each member. The SST anomalies used in the experiments were constructed by regressing tropical Pacific SST (20°S–20°N) anomalies to the EP and CP El Niño indices and then scaled to typical El Niño magnitudes (shown in Figure 2). During the typical evolution of an EP El Niño event, warm SST anomalies first appear south of the equator, near the South American coast, then extend northward toward the equatorial cold tongue, and eventually spread westward into the central equatorial Pacific. As for a typical CP El Niño event, the warming appears first in the northeast subtropical Pacific and then extends into the central equatorial Pacific. After SST anomalies have been established at the
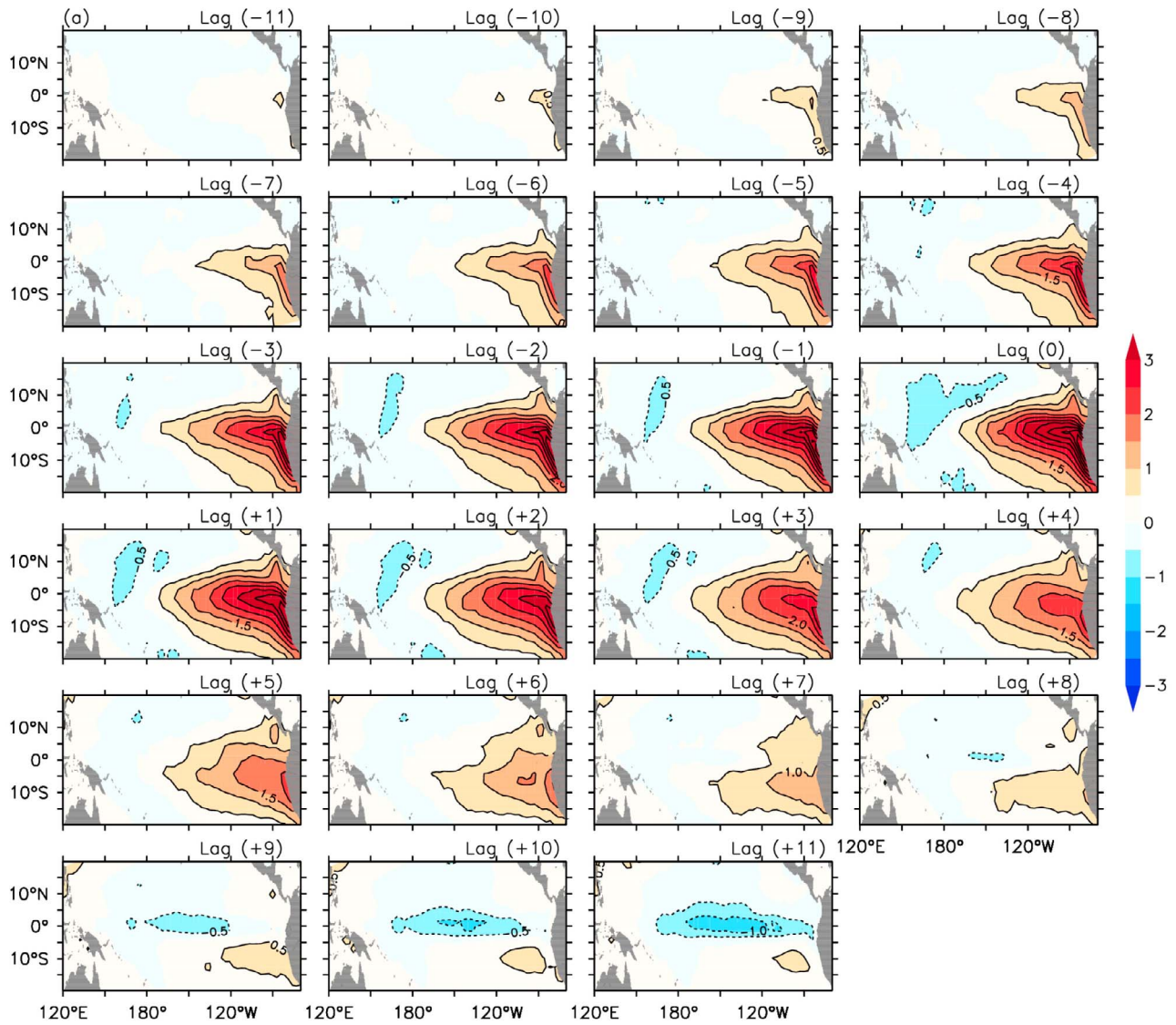
Figure 2. SST anomalies regressed onto the (a) EP and (b) CP El Niño index, from 11 months before to 11 months after the peak of the index. The values shown are the regression coefficients scaled by a factor of 4.5. Contour intervals are 0.5°C.
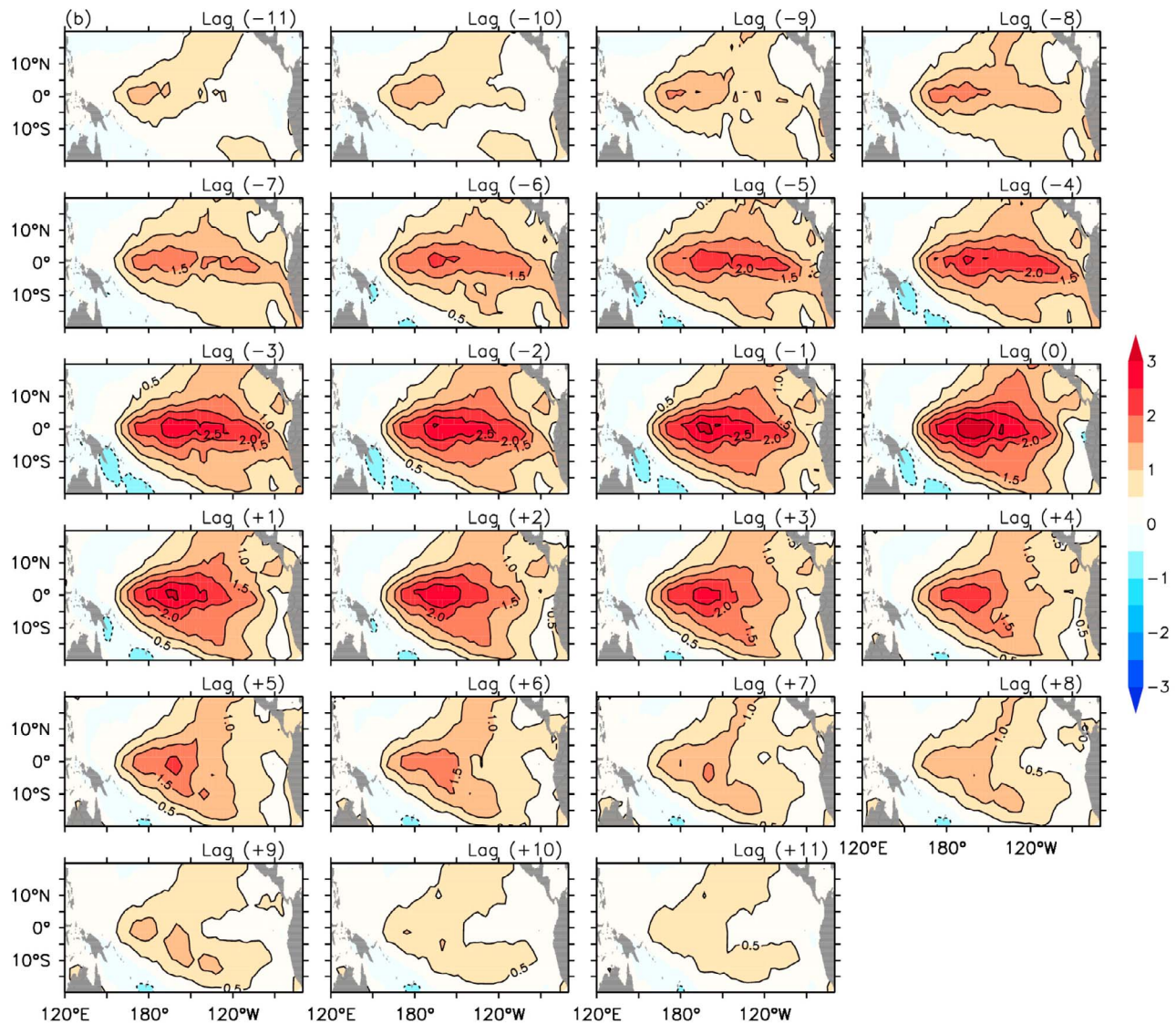
Figure 2. (continued)

equator, the warming intensifies rapidly with the anomalies extending eastward, but remaining detached from the South American Coast.

[8] The impacts produced by the EP and CP types of El Niño in the model experiments were identified by subtracting the ensemble mean of the control run from the ensemble means of the EP and CP runs (Figure 3). It is very encouraging to find that the regressed winter US impact patterns produced by the EP and CP types of El Niño in the observations were reproduced in the forced model
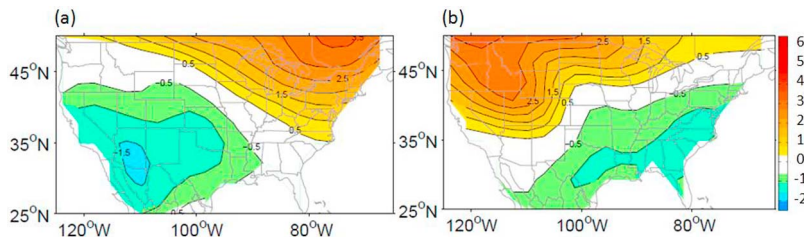

Figure 3. Results from the forced model experiments showing winter (JFM) near-surface air temperature differences between the (a) ensemble mean of the EP run and that of the control run and (b) ensemble mean of the CP run and that of the control run. Contour intervals are 0.5°C. Only the differences that are statistically significant (at the 90% level) based on the student-t test are colored.

Table 1. Major El Niño Events Since 1950 and Their Types Identified by the Majority Consensus From the EP/CP-Index Method, the Niño Method, and the EMI Method

| | El Niño Years | Type | | | |
		EP/CP method	Niño3/4 method	EMI method	Consensus
1	1951–52	EP	EP	EP	EP
2	1953–54	CP	CP	EP	CP
3	1957–58	CP	EP	CP	CP
4	1958–59	CP	CP	CP	CP
5	1963–64	CP	CP	CP	CP
6	1965–66	CP	EP	CP	CP
7	1968–69	CP	CP	CP	CP
8	1969–70	CP	EP	EP	EP
9	1972–73	EP	EP	EP	EP
10	1976–77	EP	EP	EP	EP
11	1977–78	CP	CP	CP	CP
12	1982–83	EP	EP	EP	EP
13	1986–87	CP	EP	EP	EP
14	1987–88	CP	CP	EP	CP
15	1991–92	CP	EP	CP	CP
16	1994–95	CP	CP	CP	CP
17	1997–98	EP	EP	EP	EP
18	2002–03	CP	EP	CP	CP
19	2004–05	CP	CP	CP	CP
20	2006–07	EP	EP	EP	EP
21	2009–10	CP	CP	CP	CP

experiments. The CAM4 model produces a warm-northeast, cold-southwest anomaly pattern in surface air temperatures when the model is forced by SST anomalies of the EP El Niño. The same model produces a warm-northwest, cold-southeast anomaly pattern when it is forced by the SST anomalies of the CP El Niño. The centers of the winter temperature anomalies coincide reasonably well with the regression results based on observations (Figure 1).

[9] To further demonstrate the robustness of the different impacts obtained with the regression analysis and the model experiments, we also examined event-by-event the US winter temperature anomalies observed during all major El Niño events since 1950. Here, the El Niño events were selected based on NOAA's criterion that the Ocean Niño Index (ONI) be greater than or equal to 0.5°C for a period of at least five consecutive and overlapping three-month seasons. A total of 21 events are identified based on the ONI index and are listed in Table 1. We then determined the type of these 21 El Niño events based on the consensus of three identification methods, which include the EP/CP-index method of *Kao and Yu* [2009], the Niño method of *Yeh et al.* [2009], and the El Niño Modoki index (EMI) method of *Ashok et al.* [2007]. Using the EP/CP-index method, the events in Table 1 were classified as CP types when the December–January–February (DJF)-averaged values of the CP index were greater than those of the EP index, and vice versa for EP types. With the Niño method, El Niño events were classified as CP (EP) types when the DJF-averaged values of the Niño4 index were greater (less) than the averaged values of the Niño3 index. With the EMI method, El Niño events were considered to be the CP type when the values of the DJF averaged EMI were equal to or greater than 0.7 STD. Here STD is the DJF standard deviation (0.46) of the EMI. To maintain consistency in the analyses, the identification of El Niño types by the EMI method were based on the DJF averages, although *Ashok et al.* [2007] used both June–July–August–September (JJAS) and DJF averages.

[10] According to the majority consensus of Table 1, eight of the 21 major El Niño events are of the EP type, and thirteen of them are of the CP type. Figure 4 shows the US winter (JFM) temperature anomalies during these two groups of El Niño events. Since US winter temperatures can be affected by factors other than El Niño (e.g., remote forcing from SST variations in the Atlantic Ocean, local land surface processes, and the internal dynamics of the atmosphere), the impact patterns of El Niño on US temperatures should be more detectable during strong El Niño events than weak events. Therefore, we display the US winter temperature anomalies in Figure 4 in order from the strongest to the weakest events. The intensity of the events are determined based on the value of the Niño3 (Niño4) SST index for the EP (CP) El Niño. For the EP El Niños, the warm-northeast, cold-southwest impact pattern on US winter temperatures can be identified in the four strongest events, which include the 1997, 1982, 1972, and 1986 El Niño events. For the CP El Niño, the warm-northwest, cold-southeast impact pattern can be identified in four of the top five strongest events: the 2009, 1957, 2002, and 2004 events, a group that includes most of the El Niño events in the 21st century. The event-by-event examination presented here further demonstrates that the EP and CP types of El Niño produce different impacts on US winter temperatures.

[11] Why would these two types of El Niño produce different impacts on US winter temperatures? A regression analysis with the EP and CP El Niño indices reveals that in association with CP El Niño events (Figure 5a), the winter atmosphere produces an anomaly pattern of 500 mb geopotential height that resembles the Pacific/North American teleconnection (PNA) [*Wallace and Gutzler*, 1981] pattern. This pattern consists of a positive anomaly center extending from eastern Alaska to northwestern US and a negative anomaly center over southeastern US, resulting in a warm-northwest, cold-southeast pattern of temperature anomalies. However, such a PNA-like pattern does not appear in the winter atmosphere during EP El Niño events (Figure 5b). The anomaly pattern of the 500 mb geopotential heights in this case is characterized by a poleward wave train emanating from the tropical eastern Pacific, across the southwestern US, and into the northeastern US, leading to the cold-southwest, warm-northeast pattern in US winter temperatures. These anomaly patterns of the atmospheric response are further confirmed in the EP and CP runs conducted with the CAM4 model. As shown in Figures 5c and 5d, when the CAM4 model is forced by CP El Niño anomalies, the winter atmosphere produces a PNA anomaly pattern in 500 mb geopotential heights, but a poleward wave train is produced when the model is forced by the EP El Niño. To further verify that the impact of the CP El Niño on US winter temperatures is truly associated with the PNA pattern, we also calculated the regression of the US winter temperatures to the PNA index (downloaded at http://www.cpc.ncep.noaa.gov/products/precip/CWlink/pna/pna.shtml) using both the NCEP-NCAR reanalysis and the CAMS dataset and found the regression pattern (see Figure S1 in the auxiliary material) similar to the pattern shown in Figure 5a.[1] Also, the correlation coefficient between the PNA index and the CP Index is larger (i.e., 0.43

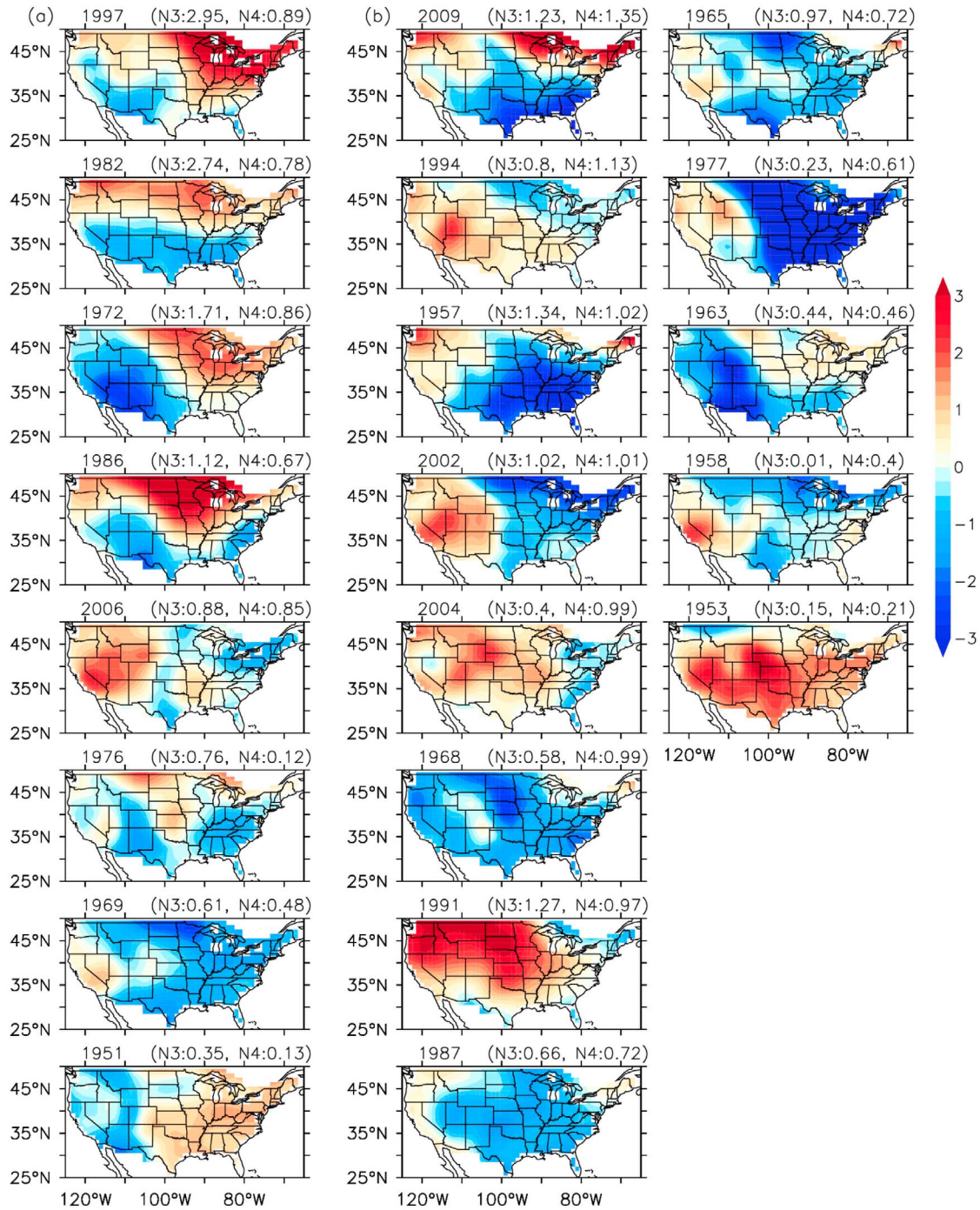[1]Auxiliary materials are available in the HTML. doi:10.1029/2012GL052483.

Figure 4. US winter (JFM) surface air temperature anomalies (°C) during (a) eight EP El Niño events and (b) thirteen CP El Niño events. Values of the DJF-averaged Niño3 (N3) and Niño4 (N4) SST indices for each event are displayed in parentheses.
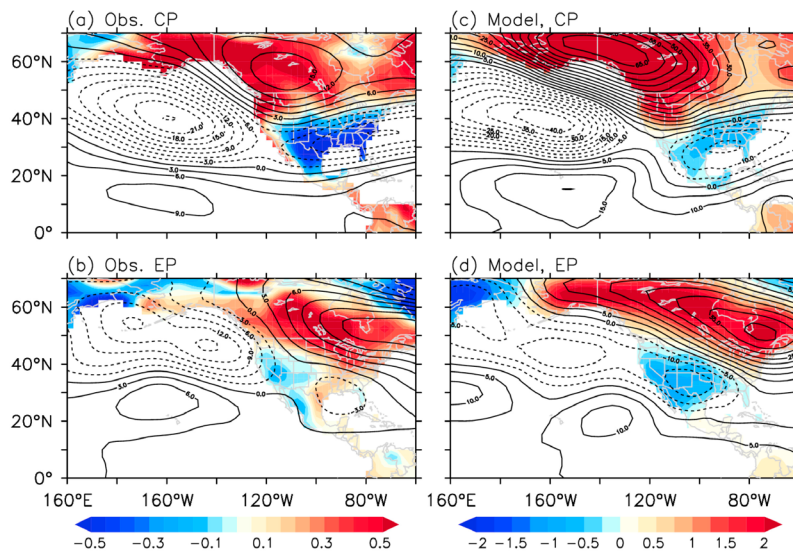
Figure 5. Observed anomalies of 500 mb geopotential heights (contours) and surface air temperatures (color shade) regressed with the (a) CP and (b) EP indices, and the JFM-averaged near-surface air temperature and 500 mb geopotential height differences (c) between the ensemble means of the CP run and the control run and (d) between the ensemble mean of the EP run and that of the control run.

for JFM means) than that between the PNA index and the EP Index (i.e., 0.24).

4. Conclusions

[12] We have demonstrated that the EP and CP types of El Niño have different impacts on US winter surface air temperatures and have identified the regions of the US that are most sensitive to each type of El Niño. Based on this view, the recent emergence of the CP type of El Niño implies that the impact of El Niño on US winter temperature could become more pronounced over the northwestern and southeastern US than any other part of the country. Our results refine the classical view of El Niño impact and provide a framework for more accurate predictions of its effects on the US. Our findings also have important implications on how the El Niño will influence US climate in the future, should the occurrence of the CP type of El Niño continue to rise in response to climate change [*Yeh et al.*, 2009; *Kim and Yu*, 2012].

[14] The Editor thanks the two anonymous reviewers for assisting in the evaluation of this paper.

References

Alexander, M. A., I. Bladé, M. Newman, J. R. Lanzante, N.-C. Lau, and J. D. Scott (2002), The atmospheric bridge: The influence of ENSO teleconnections on air–sea interaction over the global oceans, *J. Clim.*, 15, 2205–2231, doi:10.1175/1520-0442(2002)015<2205:TABTIO>2.0. CO;2.

Ashok, K., S. K. Behera, S. A. Rao, H. Weng, and T. Yamagata (2007), El Niño Modoki and its possible teleconnection, *J. Geophys. Res.*, 112, C11007, doi:10.1029/2006JC003798.

Barsugli, J. J., and P. D. Sardeshmukh (2002), Global atmospheric sensitivity to tropical SST anomalies throughout the Indo-Pacific Basin, *J. Clim.*, 3427–3442, doi:10.1175/1520-0442(2002)015<3427:GASTTS> 2.0.CO;2.

DeWeaver, E., and S. Nigam (2004), On the forcing of ENSO teleconnections by anomalous heating and cooling, *J. Clim.*, 3225–3235, doi:10.1175/1520-0442(2004)017<3225:OTFOET>2.0.CO;2.

Hoerling, M., and A. Kumar (2003), The perfect ocean for drought, *Science*, 299, 691–694, doi:10.1126/science.1079053.

Kao, H.-Y., and J.-Y. Yu (2009), Contrasting eastern-Pacific and central-Pacific types of ENSO, *J. Clim.*, 22, 615–632, doi:10.1175/ 2008JCLI2309.1.

Kim, S. T., and J.-Y. Yu (2012), The two types of ENSO in CMIP5 models, *Geophys. Res. Lett.*, 39, L11704, doi:10.1029/2012GL052006.

Kistler, R. E., et al. (2001), The NCEP-NCAR 50-year reanalysis: Monthly means CD-ROM and documentation, *Bull. Am. Meteorol. Soc.*, 82, 247–267, doi:10.1175/1520-0477(2001)082<0247:TNNYRM>2.3.CO;2.

Kug, J.-S., F.-F. Jin, and S.-I. An (2009), Two types of El Niño events: Cold Tongue El Niño and Warm Pool El Niño, *J. Clim.*, 22, 1499–1515, doi:10.1175/2008JCLI2624.1.

Larkin, N. K., and D. E. Harrison (2005a), Global seasonal temperature and precipitation anomalies during El Niño autumn and winter, *Geophys. Res. Lett.*, 32, L16705, doi:10.1029/2005GL022860.

Larkin, N. K., and D. E. Harrison (2005b), On the definition of El Niño and associated seasonal average U.S. weather anomalies, *Geophys. Res. Lett.*, 32, L13705, doi:10.1029/2005GL022738.

Lee, T., and M. J. McPhaden (2010), Increasing intensity of El Niño in the central-equatorial Pacific, *Geophys. Res. Lett.*, 37, L14603, doi:10.1029/ 2010GL044007.

Mo, K. C. (2010), Interdecadal modulation of the impact of ENSO on precipitation and temperature over the United States, *J. Clim.*, 23, 3639–3656, doi:10.1175/2010JCLI3553.1.

Mo, K. C., and R. W. Higgins (1998), The Pacific–South American modes and tropical convection during the Southern Hemisphere winter, *Mon. Weather Rev.*, 126, 1581–1596, doi:10.1175/1520-0493(1998) 126<1581:TPSAMA>2.0.CO;2.

Ropelewski, C. F., and M. S. Halpert (1986), North America precipitation and temperature associated with the El Niño/Southern Oscillation (ENSO), *Mon. Weather Rev.*, 114, 2352–2362, doi:10.1175/1520-0493 (1986)114<2352:NAPATP>2.0.CO;2.

Ropelewski, C. F., J. E. Janowiak, and M. S. Halpert (1984), The Climate Anomaly Monitoring System (CAMS), report, 39 pp., Clim. Anal. Cent., NWS, NOAA, Washington, D. C.

Smith, T. M., and R. W. Reynolds (2003), Extended reconstruction of global sea surface temperatures based on COADS data (1854–1997), *J. Clim.*, 16, 1495–1510, doi:10.1175/1520-0442-16.10.1495.

Trenberth, K., and D. P. Stepaniak (2001), Indices of El Niño evolution, *J. Clim.*, 1697–1701, doi:10.1175/1520-0442(2001)014<1697:LIOENO> 2.0.CO;2.

Wallace, J. M., and D. S. Gutzler (1981), Teleconnections in the potential height field during the Northern Hemisphere winter, *Mon. Weather*

Rev., *109*, 784–812, doi:10.1175/1520-0493(1981)109<0784:TITGHF> 2.0.CO;2.

Wang, C., and R. H. Weisberg (2000), The 1997–98 El Niño evolution relative to previous El Niño events, *Phys. Oceanogr.,13*, 488–501, doi:10.1175/1520-0442(2000)013<0488%3ATENOER>2.0.CO%3B2.

Yeh, S.-W., J.-S. Kug, B. Dewitte, M.-H. Kwon, B. P. Kirtman, and F.-F. Jin (2009), El Niño in a changing climate, *Nature*, *461*, 511–514, doi:10.1038/nature08316.

Yu, J.-Y., and H.-Y. Kao (2007), Decadal changes of ENSO persistence barrier in SST and ocean heat content indices: 1958–2001, *J. Geophys. Res.*, *112*, D13106, doi:10.1029/2006JD007654.

Yu, J.-Y., and S. T. Kim (2010), Identification of central-Pacific and eastern-Pacific types of ENSO in CMIP3 models, *Geophys. Res. Lett.*, *37*, L15705, doi:10.1029/2010GL044082.